IEEE Access
Multidisciplinary | Rapid Review | Open Access Journal

Received April 13, 2021, accepted April 27, 2021, date of publication April 29, 2021, date of current version May 7, 2021.

Digital Object Identifier 10.1109/ACCESS.2021.3076683

Arrhythmia Classification Using Biased Dropout and Morphology-Rhythm Feature With Incremental Broad Learning

JIA LI[1], YANG ZHANG[2], LE GAO[1], AND XIANG LI[3], (Member, IEEE)

[1]Department of Intelligent Manufacturing, Wuyi University, Jiangmen 529020, China
[2]Department of Mechanical Engineering, Zhuhai College of Jilin University, Zhuhai 519041, China
[3]Department of Computer Science and Technology, Zhuhai College of Jilin University, Zhuhai 519041, China

Corresponding author: Jia Li (lijia14@mails.jlu.edu.cn)

This work was supported in part by the Wuyi University Hong Kong Macao Joint Research and Development under Grant 2019WGALH23, in part by the Science and Technology Project of Basic and Theoretical Scientific Research in Jiangmen City under Grant 2020JC01037, in part by the Startup Funds for Scientific Research of High-level Talents of Wuyi University under Grant 2019AL020, in part by the Guangdong Province Universities Innovation Development Project under Grant 2019CXKYTD001, and in part by the 2020 School Innovation Ability Cultivation Project under Grant 2020XJCQ004.

ABSTRACT In recent times, people have become increasingly health-conscious. To obtain timely and accurate information on the status of the heart, one of the most important organs of the human body, there is a growing demand among individuals and doctors for accurate and real-time automatic classification of arrhythmias. Consequently, this paper proposes a fast and accurate classification method for arrhythmias. In the proposed method, we build an incremental broad learning (IBL) classification model based on the biased dropout technique for arrhythmia-type recognition. In particular, we extract the morphological-rhythm features of the denoised signal as the input data of the IBL model in the electrocardiogram signal preprocessing. The IBL model enhances the classification effect of the node optimization model by using improved features. To the best of our knowledge, this study is the first application of the IBL model to the study of arrhythmia classification. The results of experiments conducted on the MIT-BIH database indicate that the proposed method is effective and achieves superior classification results. The average classification accuracy for six types of arrhythmias was 99%, and the training time required was only 2.7 s. In addition, based on the evaluation index recommended by the ANSI/AAMI EC57:2012 standard, our method is superior to existing methods on all indexes, except for the positive predictive rate of ventricular ectopic beats. Therefore, the proposed classification method outperforms state-of-the-art methods in terms of real-time performance and accuracy and provides a new approach for further improvements in arrhythmia classification.

INDEX TERMS Arrhythmia classification, biased dropout, broad learning, electrocardiogram, morphology-rhythm feature.

I. INTRODUCTION

As an important application of computers in clinical practice, automatic classification of arrhythmia can effectively prevent cardiovascular disease and is conducive to the rational allocation of medical resources. As people become increasingly health-conscious, they want to obtain timely and accurate information regarding the health status of the heart. Thus, individuals and doctors have higher requirements for the diagnosis quality of automatic classification of arrhythmias. Our study focuses on improving the detection of arrhythmias, resulting in intelligent and more meaningful computer diagnosis results. The improvement in detection ability and the provision of intelligent results are problems that need to be solved for the development of telemedicine, digital medicine, and home self-help diagnosis.

In recent years, deep neural networks have been successfully introduced for the development of intelligent, rapid, and high-precision automatic arrhythmia classification that considers diverse detection parameters [1]–[3]. For example, Fakheraldin *et al.* [4] constructed a convolutional neural network (CNN) with 11 layers for classification; the

The associate editor coordinating the review of this manuscript and approving it for publication was Li He.

classification accuracy of the network for 10 arrhythmia types from the MIT-BIH database was 99.84%, which is higher than the existing classification methods based on CNN. Huang *et al.* [5] proposed an intelligent electrocardiogram (ECG) classifier based on a fast compressed residual convolution neural network (FCResNet). Their method uses the maximum overlap wavelet packet transform (MOWPT) to decompose ECG signals. The proposed deep learning classifier can considerably alleviate the problems of low computational efficiency, difficult convergence, and model degradation. The average accuracy was 98.79% for the MIT-BIH database. Ihsanto *et al.* [6] proposed a fast and accurate algorithm for ECG authentication using residual depth-wise separable convolutional neural networks. They reported that the proposed algorithm achieved 100% accuracy when evaluated using data for 48 patients in the MIT-BIH database and 90 people in the ECG ID database. Rahhal *et al.* [7] designed a heartbeat classification algorithm based on a deep neural network (DNN). The core concept of this model involved adding a reconstruction layer on top of the hidden layer in the network, in which the activation function is a softmax function. Their experimental results showed that the algorithm not only reduces expert interaction and speeds up online retraining but also has greater robustness and higher computational efficiency. Moreover, compared with the traditional shallow neural network, it could effectively improve the heartbeat recognition effect.

Considering the morphological and rhythmic characteristics of a heartbeat, Zhang *et al.* [8] combined the recurrent neural network (RNN) and density clustering technology for arrhythmia classification; they achieved a significant recognition effect on the MIT-BIH arrhythmia database. To further improve the classification performance of the RNN, Wang *et al.* [9] used a global RNN (GRNN) to classify the heartbeat, with the heartbeat having the largest amount of information being selected through GRNN's self-learning method. The advantages of GRNN in capacity and fitting ability were fully utilized to recognize heartbeats from different patients, which shows the good generalization ability of the algorithm.

Algorithms for automatic arrhythmia classification based on DNNs can autonomously learn the implicit features of a heartbeat through a neural network with multiple hidden layers, which is helpful in improving heartbeat recognition. However, there are numerous parameters in a DNN, such as hidden layers with multiple neurons, leading to increased training costs. Furthermore, the complexity of such networks makes it difficult to analyze the deep structure theoretically. However, to obtain a higher classification accuracy, the DNN depends on increasing the number of hidden layers in the network. To solve the aforementioned problem, Chen and Liu [10] proposed a broad learning system (BLS); specifically, a random vector functional link neural network. Such neural networks utilize a pseudo-inverse to calculate the weights of feature nodes and enhancement nodes rather than updating the feature kernel with backpropagation. Compared with deep learning-based image classification (for example, for skin cancer diagnosis), BLS is more suitable for arrhythmia discrimination because the heartbeat contains fewer features than medical images. Moreover, the coupling within layers disappears in BLS, and the updating of weights does not depend on the gradient descent method, which significantly saves time in the training process. Conversely, the scalability of the network is high as the remodeling can be realized by an incremental learning algorithm without training the entire network.

Thus, it is clear that deep learning has been successfully used to solve some problems related to arrhythmia classification and feature extraction. However, the complex structure of a deep learning network with multiple hidden layers increases training time and causes poor real-time performance of the classification model. To solve the above problems, we applied the incremental broad learning (IBL) model to the automatic classification of arrhythmias. To the best of our knowledge, this is the first attempt to apply the IBL model to arrhythmia classification.

This study was conducted with the aim of further improving the performance of arrhythmia classification using IBL. In addition, to solve the problem of redundancy due to the network expansion of IBL, this study uses the target deactivation technology as a new regularization method to optimize the model in a single hidden layer of IBL, and further reduces the training time cost by purposefully deactivating some neuron nodes.

The remainder of this paper is structured as follows. Section II discusses biased dropout technology and Section III gives an overview of broad learning. Section IV describes the proposed classification method. Section V outlines the experiments conducted and analyzes the results obtained. Finally, Section VI presents concluding remarks.

II. BIASED DROPOUT

Biased dropout [11] is an extension of the random dropout technology. It is a process that changes the structure of a neural network to avoid overfitting, which may occur when training a model with many neurons. Unlike standard dropout, which is biased by randomly deactivating partial nodes and connections, the biased dropout is biased by purposely deactivating partial neurons and connections. Poernomo and Kang [11] showed that, compared with classic dropout, this purposeful dropout technique can not only avoid overfitting but also improve the learning ability and training rate of the network model, especially when the number of learning samples is limited. With this analysis in mind, in this study, biased dropout acts on a single hidden layer of the IBL to optimize the model further.

Fig. 1 shows the neuron inactivation in the network after dropout and biased dropout. As shown in Fig. 1(a), when the inactivation rate p is 0.5, half of the neurons are inactivated; these neurons are randomly selected without considering the contribution of individual neurons to the network. Unlike standard dropout, biased dropout takes into account how

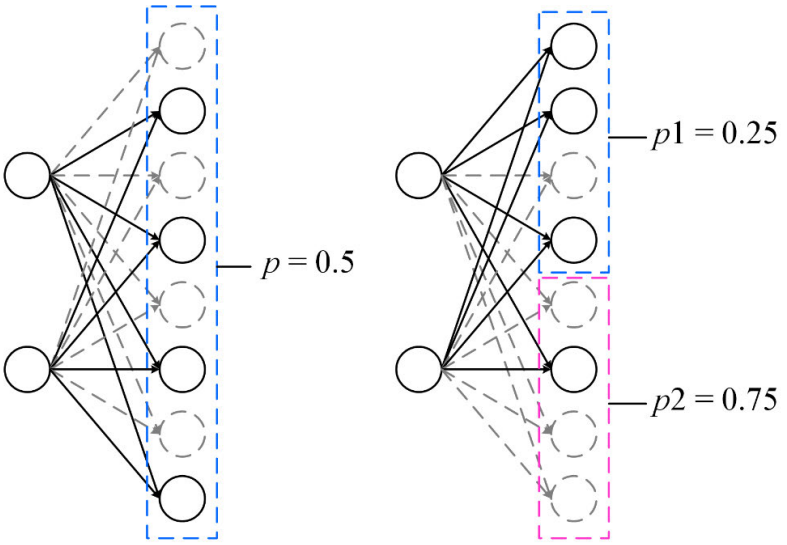

（a）Neural network using Dropout technology

（b）Neural network using Biased Dropout technology

FIGURE 1. Neuron inactivation using different dropout techniques.

much each neuron contributes to the network. This technology sorts and groups all neurons according to their contribution to the network, and then performs a dropout operation. As shown in Fig. 1(b), first, the contribution values of the neurons in the network are sorted from large to small. The blue areas represent the contribution values of the top 50% of neurons, whereas the red areas represent those of the bottom 50%. Subsequently, according to the inactivation rate p2 (p1 < p2), neurons with the smallest contribution values in the red area are progressively deactivated, ultimately achieving the goal of retaining those neurons with the larger contribution values.

The inactivation rate of the hidden layer output neuron is usually inversely proportional to its contribution to network performance. In the specific hidden layer output, when the number of neurons (x^l) is n, the neurons are divided into two groups according to the large or small contribution to the network of neurons, which is represented by x^l (1) and x^l (2), respectively. Moreover, $p1$ represents the inactivation rate of those neurons with a large contribution, and p2 represents that of those with a small contribution. The contribution size refers to the size of the neuron's own value. The relationship between p1 and p2 is shown in (1), and (2) is used to calculate the average inactivation rate p. Equation (3) is used to convert the inactivation rate of the output neurons at layer l in the network into a Bernoulli distribution [125].

$$p2 = c \times p1 (c > 1) \tag{1}$$

$$p = \frac{(p1 \times x^l(1) + p2 \times x^l(1))}{n} \tag{2}$$

$$r \sim \text{Bernoulli}\ (p) \tag{3}$$

Finally, (4) and (5) are used to map the output neurons of layer L. These equations show the output neurons after the biased dropout is applied.

$$\tilde{x}^l = r^l \times x^l \tag{4}$$

$$x^{l+1} = f(\mathrm{W}\tilde{x}^l + b^{l+1}) \tag{5}$$

III. BROAD LEARNING

The structure of broad learning for arrhythmia classification is shown in Fig. 2. The input data X are obtained from the sample set representing different arrhythmia types, and the sample length of each sample set is M. The mapping of the input data Z_i can be represented as

$$Z_i = XW_{ei}, \tag{6}$$

where i is the set number and W_{ei} is the weight for each sample set, which is generated randomly. The former i sets of the mapped data can be expressed as $Z^i = [Z_1, Z_2, \ldots, Z_i]$. By transforming the mapped features of Z_i we obtain the enhancement modes H_j, which are denoted as

$$H_j = \xi\left([Z_1, Z_2, \ldots, Z_i]\, W_{hj} + \beta_{hj}\right), \tag{7}$$

where W_{hj} and β_{hj} are the weights and biases generated randomly. ξ is the activation function; the former j sets of enhancement nodes are expressed as $H^j = [H_1, H_2, \ldots, H_j]$. In this way, all the mapped feature nodes and the enhancement nodes are represented as $Z^n = [Z_1, \ldots, Z_n]$ and $H_m = [H_1, \ldots, H_m]$, respectively. Finally, all the mapped feature nodes and enhancement nodes are connected to the output, yielding Y:

$$\begin{aligned} Y &= \left[Z_1, \ldots, Z_n | \xi\left(Z^n W_{h1} + \beta_{h1}\right), \ldots,\right. \\ &\quad \left. \times \xi\left(Z^n W_{hm} + \beta_{hm}\right)\right] W^m \\ &= [Z_1, \ldots, Z_n]\,[H_1, \ldots, H_m]\, W^m = \left[Z^n | H^m\right] W^m, \end{aligned} \tag{8}$$

where the operation | merges Z^n and H^m to a line.

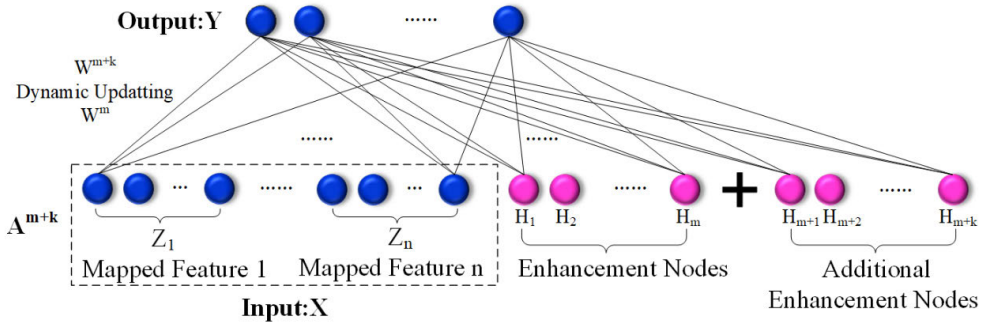

FIGURE 2. Structure of broad learning for the arrhythmia classification task.

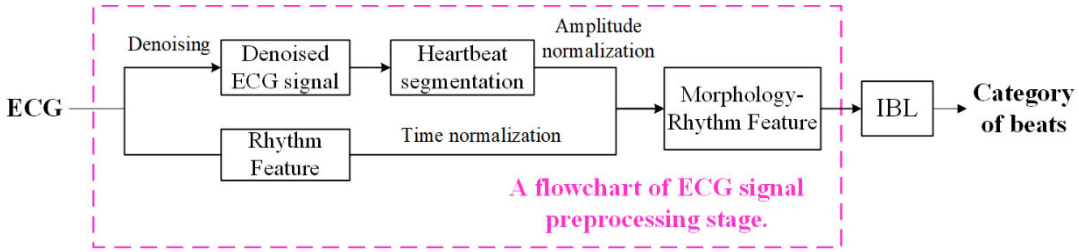

FIGURE 3. Classification process.

The classification accuracy is improved by increasing the number of enhancement nodes. Assuming the original input matrix,

$$A^m = \left[Z^n | H^m\right], \tag{9}$$

the new matrix can be represented as

$$\begin{aligned} A^{m+k} &= \left[A^m | H_{m+q}\right] \\ &= \left[A^m | \xi\left(\left[Z_1, Z_2, \ldots, Z_n\right] W_{m+q}\right)\right], \quad q = 1, 2, \ldots, k, \end{aligned} \tag{10}$$

where q is the additional enhancement nodes, which equals k. w_{m+q} is the randomly generated weight for all enhancement nodes. Thus, the pseudo-inverse of the new matrix A^{m+k} can be represented as

$$\left(A^{m+k}\right)^+ = \begin{bmatrix} (A^m)^+ - DB^T \\ B^T \end{bmatrix}, \tag{11}$$

where

$$D = \left(A^m\right)^+ \xi\left(\left[Z_1, Z_2, \ldots, Z_n\right] W_{m+q}\right) \tag{12}$$

and

$$\begin{aligned} B^T &= \begin{cases} (C)^+, & C \neq 0 \\ \left(1 + D^T D\right)^{-1} B^T \left(A^m\right)^+, & C = 0 \end{cases} \\ C &= \xi\left(\left[Z_1, Z_2, \ldots, Z_n\right] W_{m+q}\right) - A^m D. \end{aligned} \tag{13}$$

The pseudo-inverse of the new matrix A^{m+k} is calculated with ridge regression,

$$\left[Z^n | H^m\right]^+ = \lim_{\lambda \to 2} \left(\lambda I + \left[Z^n | H^m\right]\left[Z^n | H^m\right]^T\right)^{-1} \left[Z^n | H^m\right]^T, \tag{14}$$

where λ is the regularization norm. Therefore, the weight of the enhancement notes is updated as

$$W^{m+q} = \begin{bmatrix} W^m - DB^T Y \\ B^T Y \end{bmatrix}, \tag{15}$$

rather than calculating the pseudo-inverse of the new matrix A^{m+k}.

IV. CLASSIFICATION METHOD

Fig. 3 shows the classification process proposed in this paper, including the two stages of ECG signal preprocessing and classification. First, the ECG signals are processed in two ways. On the one hand, the morphological feature of each heartbeat signal is obtained after the segmentation of the denoised signals; on the other hand, the rhythm feature between heartbeats is extracted. Subsequently, the aforementioned features are fused to obtain morphology-rhythm features as the input of the proposed IBL model (Fig. 2). Finally, the heartbeat type is identified.

A. PREPROCESSING

The human ECG signal is a nonlinear and nonstationary weak signal with an amplitude of millivolts. This weak signal is easily affected by environmental noise and other factors. To remove the baseline drift noise and high-frequency noise of the ECG signal, we combine the median filter and wavelet transform to obtain high-quality signals.

First, we use the parameters for 50 levels of the median filter to the original ECG signal to obtain a set of baseline drifts or noise, employing parameters for 150 orders of the median filter. These steps are repeated to obtain another set of baseline drifts, and we obtain the original ECG signal minus

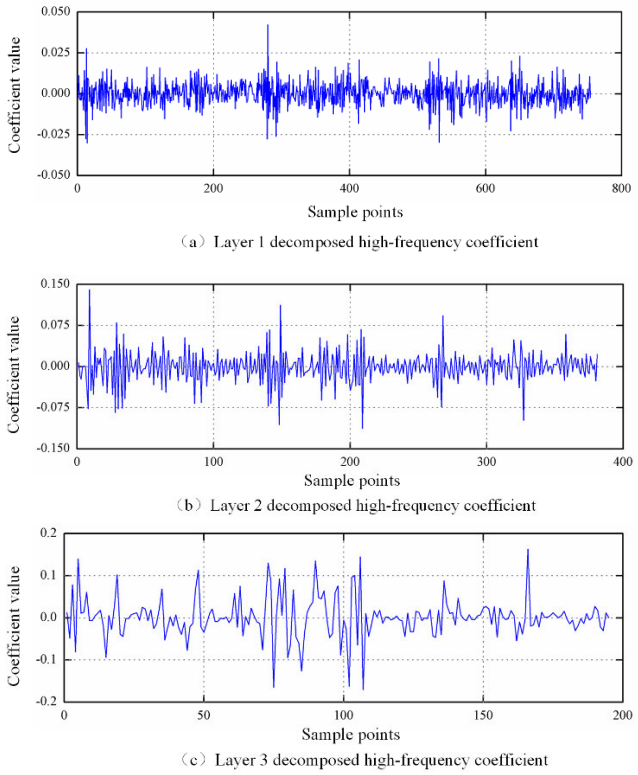

FIGURE 4. High-frequency coefficients of each layer after wavelet decomposition.

the aforementioned two groups of baseline noise; finally, we filter out the noise of the ECG signal baseline drift.

Next, after removing the baseline drift noise, the signal is decomposed by a three-layer wavelet; the Daubechies (DB) 5 wavelet is selected as the parent wavelet. The high-frequency coefficients of the different layers are obtained as shown in Fig. 4. Then, the thresholds of the high-frequency coefficients of each layer after decomposition are determined by using the unbiased likelihood estimation method. Subsequently, the soft threshold method is used to carry out threshold quantization processing on the high-frequency coefficients to obtain high-frequency information.

Finally, the low-frequency coefficient of the third layer, after wavelet decomposition, and the high-frequency information of each layer after threshold processing are reconstructed to obtain the ECG signal after filtering the high-frequency noise.

The denoised ECG signal is processed in two treatments. The duration of each wave (for example, the P-wave) is approximately 0.08–0.11 s, and the cycle of a complete heartbeat is approximately 0.65 s. Thus, we extract 234 (0.65 s × 360 Hz) sample points, centering on the peak of the R-wave. Then, we downsample each segmented heartbeat to 97 sample points as the morphological feature of the heartbeat signal. As arrhythmia always induces an abnormal duration between the R-R interval, we use three R-R-wave-related variables (RR_{pre}, RR_{pos}, RR_{diff}) as the rhythm feature. RR_{pre} is

TABLE 1. Number of beats for the sample set.

Class	N	/	A	V	L	R	Total
Training set	3600	2170	1488	4006	4842	5916	22022
Testing set	2400	1446	992	2640	3227	1366	12071

the R-R interval between the current peak of the R-wave and the former wave, whereas RR_{pos} is the R-R interval between the current peak of the R-wave and the latter wave. RR_{diff} is the difference between RR_{pre} and RR_{pos}. Finally, the three variables are normalized to [0, 1] and concatenated to the sampled 97 points as the extracted morphology-rhythm feature.

B. CLASSIFICATION

In this study, we constructed an IBL model (Fig. 2) as a classifier to identify arrhythmia types, and improved the classification effect by changing the structure of the model in the enhancement nodes of each reinforcement learning.

The parameters of IBL were determined during cross-validation as follows. As shown in Fig. 2, the number of windows of the feature nodes is 20, the number of enhancement nodes is 200, and the number of enhancement nodes in each incremental learning is 400. Here, "20" signifies that the number of packets captured is 20, corresponding to the number of neurons contained in label Z in Fig. 2. The figure "200" refers to the number of neurons introduced into the network at the beginning, corresponding to the red circle labeled "Additional Enhancement Nodes"; that is, m in H_m is set to 200. The figure "400" refers to the number of neurons used to further expand the network, corresponding to the red circle labeled "increase enhancement node" in Fig. 2, so that k in H_{m+k} is set to 400. As shown in Fig. 1, the dropout rate is 25%. Here, 25% is the proportion of enhancement nodes discarded in each incremental learning, which is 300 (i.e., 400 × (1 – 0.25)). Hence, 300 of the 400 enhancement nodes (the number of neurons with values in the top 300) are reserved for accessing the network.

C. DATABASE

The experimental data were obtained from the MIT-BIH arrhythmia database [12]. We extracted single-lead data for six arrhythmia types (modified limb lead II, MLII) from the database: normal beat (N), paced beat (/), atrial premature beat (A), premature ventricular contraction (V), left ventricular bundle branch block (L), and right bundle branch block beat (R). Because the proportion of normal heartbeats accounts for 73.3% (n = 73542) of the total samples, we randomly chose 6000 normal heartbeats for the classification. The number of beats for the sample set that contains six types of heartbeats is shown in Table 1. We randomly chose 60% of the heartbeats from the sample set as a training set. The rest of the dataset was used as the testing set.

TABLE 2. Training and testing datasets selection with AAMI recommendation.

Categories	N	SVEB	VEB	F	Q	Total
Training	47844	2181	2072	191	7	52295
Testing	42075	2535	4107	927	8	49652

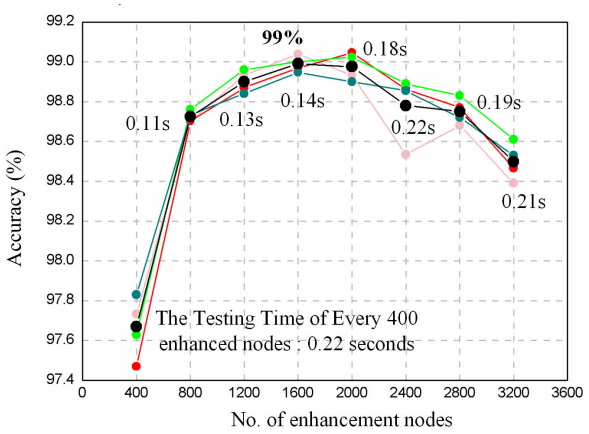

FIGURE 5. Classification accuracy with the enhancement of IBL nodes.

In addition, to objectively evaluate the classification performance of the proposed network structure, and further analyze the recognition effect of the proposed algorithm on ECG from different subjects, we processed the data in the MIT-BIH arrhythmia database in accordance with the Association for the Advancement of Medical Instrumentation (AAMI) ECAR-1987 recommended practice, that is, using the dataset classification method proposed in [15]. According to the AAMI recommendation, each category of the arrhythmia database can be grouped into five sub-categories: beats originating in the sinus mode (N), supraventricular ectopic beats (SVEB), ventricular ectopic beats (VEB), fusion beats (F), and unclassifiable beats (Q). Furthermore, the first five minutes of recordings were used as the training set, whereas the remaining twenty-five minutes were used as the testing set. The training and testing datasets are described in Table 2.

V. EXPERIMENTS AND RESULTS

This section reports three experiments conducted that validate the proposed method: (1) checking classification accuracy depending on the enhancement of IBL nodes; (2) comparing the training process of the proposed method with CNN; (3) analyzing the confusion matrix and arrhythmia-specific indicators.

A. EXPERIMENT 1

Fig. 5 shows the results of classification accuracy after adding enhancement in the IBL network. The test dataset is shown in Table 1. The colored circles (except black) in Fig. 5 represent the classification accuracy and time after four independent experiments, where the corresponding time refers to the additional time cost for each additional 400 enhancement nodes in the proposed neural network. The black circle represents the average accuracy of the four independent experiments. The results show that when the number of enhancement nodes is increased to 1600, the average classification accuracy reaches the peak (99%), and the total test time is only 0.6 s. Subsequently, every 400 additional nodes enter the saturation state, in which the classification accuracy presents a downward trend. It is worth noting that the aforementioned results need a total training time of only 0.52 s.

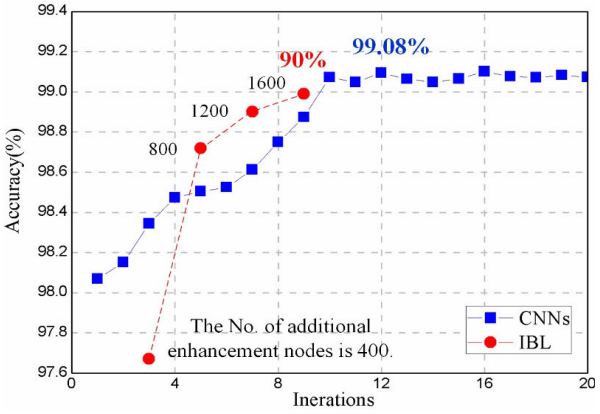

FIGURE 6. Comparison of average classification accuracy between the proposed method and CNN.

B. EXPERIMENT 2

To compare the training cost between the proposed IBL model and conventional deep learning neural network, we reproduced a classification method, CNN, which has been proposed in [13]. Fig. 6 shows the average classification accuracy curve of the two classification methods for the same dataset (Table 1). The red and blue lines represent the classification results based on IBL and CNN, respectively. The results show that the peak (99.08%) of the blue line after 12 iterations is slightly higher than that of the red line after introducing 1600 enhancement nodes (99%). In addition, considering the time cost, it only takes 0.6 s for IBL to achieve 99% classification accuracy on the test set with a training time of less than 2.7 s. By contrast, CNN requires 60 s and 2 s for training and testing, respectively, to reach the peak. Comparison of the training time cost shows that IBL completes the data learning in significantly less training time than CNN, and achieves an excellent learning effect.

C. EXPERIMENT 3

To comparatively evaluate the classification performance of our method more accurately and ensure the credibility of the experimental results, the ANSI/AAMI EC57:2012 standard [14], formulated by AAMI, was adopted in this comparative experiment. AAMI specifies the indicators used to evaluate the arrhythmia classification performance, including confusion matrix, accuracy (Acc), sensitivity (Sen), specificity (Spe), and positive prediction rate (Ppr). The

TABLE 3. Confusion matrix for recognition results of five types of beats.

Ground Truth	Classification result					
	N	SVEB	VEB	F	Q	Precision (%)
N	41947	0	117	15	0	99.7
S	0	2299	194	42	0	90.7
V	45	0	4042	20	0	98.4
F	24	0	428	475	0	51.2
Q	5	0	3	0	0	0

corresponding mathematical description is as follows:

$$Acc = \frac{TP + TN}{TP + TN + FP + FN} \tag{16}$$

$$Sen = \frac{TP}{TP + FN} \tag{17}$$

$$Spe = \frac{TN}{TN + FP} \tag{18}$$

$$Ppr = \frac{TP}{TP + FP} \tag{19}$$

where TP is true positive, TN is true negative, FP is false positive, and FN is false negative. In arrhythmia classification, accuracy represents the overall classification performance of all types of beats. In contrast, the sensitivity, specificity, and positive predictive rates are indicators that enable the evaluation of the effectiveness of recognition of the algorithm for specific types of beats.

Table 3 lists the classification results of the proposed method on the test set (Table 2) as a confusion matrix. The recall rate of other types of heartbeat reached more than 90%, except for the F and Q types. In the recognition results of SVEB cardiac beats, some of them were wrongly classified as VEB and F, resulting in low precision (90.7%); however, these results were still significantly higher than the recall results in the literature [17], [18], which were 60.31% and 76.9%, respectively. In the recognition of VEB beats, because a small number of beats were wrongly classified as N and F, the precision was 98.4%, which was higher than that of Zhai and Tin [18] (93.96%).

Table 4 presents the classification methods proposed by other authors. Table 5 summarizes the results of identifying SVEB and VEB types of beats using the methods from Table 4. Jiang and Kong [15] proposed block-based neural networks (BbNN) for beat classification, which includes modular components with a flexible structure and internal configuration. Ince *et al.* [16] used morphological wavelet transform and principal component analysis to project the beat into a low-dimensional feature space and extracted the time domain features of ECG data. They combined a feed-forward and fully connected artificial neural network with multidimensional particle swarm optimization to classify the beat. Kiranyaz *et al.* [17] used an adaptive one-dimensional CNN model for beat classification. Zhai and Tin [18] first transformed the beat into a two-beat coupling matrix as the input of a two-dimensional CNN, which captured the morphology of the ECG central beat and the R-R interval information between adjacent beats. Subsequently, they used a system-specific type of beat selection program to select representative beats for the training model.

TABLE 4. Other classification methods.

Method	Classifier
Jiang and Kong [15]	BbNN
Ince et al. [16]	Artificial neural network
Kiranyaz et al. [17]	1-dimensional CNN
Zhai and Tin [18]	2-dimensional CNN

According to the results in Table 5, the Acc, Sen, Spe, and Ppr of the proposed IBL model for VEB are 99.5%, 100%, 99.5% and 90.7%, respectively. Meanwhile, all the evaluation indexes of SVEB, except Sen, reached more than 98%. Thus, the contributions of the method are very clear. First, the proposed method shows significantly better results for the indicators of VEB than for SVEB. Second, compared with the other algorithms, the indexes of the proposed method are higher than those of the other algorithms except for the Ppr of VEB type. Specifically, SVEB's Sen and Ppr are 84.5% and 98.4%, respectively, which are lower in the other algorithms. Compared with Kiranyaz *et al.* [19] (95.0%), the result of Sen of VEB increased by 5%.

D. DISCUSSION

The results of experiments 1 and 2 show that the proposed IBL model is an effective automatic classifier of arrhythmias. Compared with the DNN model, the IBL model embedded with biased dropout technology has similar classification accuracy and higher real-time performance, especially in reducing the time of training and testing. The results above show that the t-biased dropout technique can effectively compress the number of enhancing neurons and improve the classification accuracy by purposefully selecting high-quality nodes.

The results of Experiment 3 further verify the effectiveness of the IBL. The proposed method achieved significantly better results than other algorithms in most indexes of SVEB and VEB. The reason is that the morphological-rhythm feature, extracted from ECG signal preprocessing, is helpful in characterizing the traits of the SVEB and VEB beat. In addition, the test samples in Table 2 are new data for comparative experiments, which shows that the proposed algorithm has good generalization ability for "fresh data." In addition, the IBL classifier constructed in this study deals with various small channels, and the classification algorithm works for single-lead acquisition of ECG signals, which is suitable for application in lightweight portable devices. Therefore, our study provides a technical reference for further research and development of electronic home health-monitoring and auxiliary diagnosis products.

TABLE 5. Evaluation index of different algorithms on VEB and SVEB beat types.

Methods	VEB				SVEB			
	Acc	Sen	Spe	Ppr	Acc	Sen	Spe	Ppr
Jiang and Kong [15]	98.1	86.6	99.3	**93.3**	96.6	50.6	98.8	67.9
Ince *et al.* [16]	97.6	83.4	98.1	89.5	96.1	62.1	98.5	56.7
Kiranyaz *et al.* [17]	98.6	95.0	98.1	89.5	96.4	64.6	98.6	62.1
Zhai and Tin [18]	98.6	93.8	99.2	92.4	97.5	76.8	98.7	74.0
Proposed method	**99.5**	**100**	**99.5**	90.7	**98.5**	**84.5**	**99.8**	**98.4**

Despite the achievements of our research, the generalization of the proposed automatic classification algorithm needs to be improved. For example, the proposed arrhythmia classification algorithm is only applicable to the MIT-BIH ECG database, which has certain universal significance, but it is far from universal. Therefore, in future work, we plan to design a universal automatic arrhythmia classification algorithm for other ECG databases and meet the requirements of clinical ECG signal processing.

VI. CONCLUSION

In this paper, we proposed a fast and accurate arrhythmia classification algorithm based on broad learning, and evaluated its performance on the MIT-BIH database. The BL network model promotes the update of network structure and improves the classification performance by introducing target deactivation technology and adding additional feature enhancement nodes. Therefore, we achieved a good balance between classification accuracy and training time. In addition, in the data preprocessing stage, multiangle feature extraction of ECG signal is carried out, including morphological features and rhythm features, which also plays a certain role in improving the learning ability of the model.

REFERENCES

[1] P. Xie, G. Wang, C. Zhang, M. Chen, H. Yang, T. Lv, Z. Sang, and P. Zhang, "Bidirectional recurrent neural network and convolutional neural network (BiRCNN) for ECG beat classification," in *Proc. Annu. Int. Conf. IEEE Eng. Med. Biol. Soc.*, Jul. 2018, pp. 2555–2558.

[2] U. R. Acharya, S. L. Oh, Y. Hagiwara, J. H. Tan, M. Adam, A. Gertych, and R. S. Tan, "A deep convolutional neural network model to classify heartbeats," *Comput. Biol. Med.*, vol. 89, pp. 389–396, Oct. 2017, doi: 10.1016/j.compbiomed.2017.08.022.

[3] P. Rajpurkar, A. Y. Hannun, M. Haghpanahi, C. Bourn, and A. Y. Ng, "Cardiologist-level arrhythmia detection with convolutional neural networks," 2017, *arXiv:1707.01836*. [Online]. Available: http://arxiv.org/abs/1707.01836

[4] F. Y. O. Abdalla, L. Wu, H. Ullah, G. Ren, A. Noor, H. Mkindu, and Y. Zhao, "Deep convolutional neural network application to classify the ECG arrhythmia," *Signal, Image Video Process.*, vol. 14, no. 7, pp. 1431–1439, Oct. 2020.

[5] J.-S. Huang, B.-Q. Chen, N.-Y. Zeng, X.-C. Cao, and Y. Li, "Accurate classification of ECG arrhythmia using MOWPT enhanced fast compression deep learning networks," *J. Ambient Intell. Hum. Comput.*, vol. 2, pp. 1–18, May 2020, doi: 10.1007/s12652-020-02110-y.

[6] E. Ihsanto, K. Ramli, D. Sudiana, and T. S. Gunawan, "Fast and accurate algorithm for ECG authentication using residual depthwise separable convolutional neural networks," *Appl. Sci.*, vol. 10, no. 9, p. 3304, May 2020, doi: 10.3390/app10093304.

[7] M. M. A. Rahhal, Y. Bazi, H. AlHichri, N. Alajlan, F. Melgani, and R. R. Yager, "Deep learning approach for active classification of electrocardiogram signals," *Inf. Sci., Int. J.*, vol. 345, pp. 340–354, Jun. 2016.

[8] C. Zhang, G. Wang, J. Zhao, P. Gao, J. Lin, and H. Yang, "Patient-specific ECG classification based on recurrent neural networks and clustering technique," in *Proc. IASTED Int. Conf. Biomed. Eng.*, 2017, pp. 63–67.

[9] G. Wang, C. Zhang, Y. Liu, H. Yang, D. Fu, H. Wang, and P. Zhang, "A global and updatable ECG beat classification system based on recurrent neural networks and active learning," *Inf. Sci.*, vol. 501, pp. 523–542, Oct. 2019, doi: 10.1016/j.ins.2018.06.062.

[10] C. L. P. Chen and Z. Liu, "Broad learning system: An effective and efficient incremental learning system without the need for deep architecture," *IEEE Trans. Neural Netw. Learn. Syst.*, vol. 29, no. 1, pp. 10–24, Jan. 2018, doi: 10.1109/TNNLS.2017.2716952.

[11] A. Poernomo and D.-K. Kang, "Biased dropout and crossmap dropout: Learning towards effective dropout regularization in convolutional neural network," *Neural Netw.*, vol. 104, pp. 60–67, Aug. 2018, doi: 10.1016/j.neunet.2018.03.016.

[12] G. B. Moody and R. G. Mark, "The impact of the MIT-BIH arrhythmia database," *IEEE Eng. Med. Biol. Mag.*, vol. 20, no. 3, pp. 45–50, May/Jun. 2001, doi: 10.1109/51.932724.

[13] J. Li, Y. Si, T. Xu, and S. Jiang, "Deep convolutional neural network based ECG classification system using information fusion and one-hot encoding techniques," *Math. Problems Eng.*, vol. 2018, pp. 1–10, Dec. 2018, doi: 10.1155/2018/7354081.

[14] M. Sadrawi, C.-H. Lin, Y.-T. Lin, Y. Hsieh, C.-C. Kuo, J. Chien, K. Haraikawa, M. Abbod, and J.-S. Shieh, "Arrhythmia evaluation in wearable ECG devices," *Sensors*, vol. 17, no. 11, p. 2445, Oct. 2017, doi: 10.3390/s17112445.

[15] W. Jiang and G. Seong Kong, "Block-based neural networks for personalized ECG signal classification," *IEEE Trans. Neural Netw.*, vol. 18, no. 6, pp. 1750–1761, Nov. 2007, doi: 10.1109/TNN.2007.900239.

[16] T. Ince, S. Kiranyaz, and M. Gabbouj, "A generic and robust system for automated patient-specific classification of ECG signals," *IEEE Trans. Biomed. Eng.*, vol. 56, no. 5, pp. 1415–1426, May 2009, doi: 10.1109/TBME.2009.2013934.

[17] S. Kiranyaz, T. Ince, and M. Gabbouj, "Real-time patient-specific ECG classification by 1-D convolutional neural networks," *IEEE Trans. Biomed. Eng.*, vol. 63, no. 3, pp. 664–675, Mar. 2016, doi: 10.1109/TBME.2015.2468589.

[18] X. Zhai and C. Tin, "Automated ECG classification using dual heartbeat coupling based on convolutional neural network," *IEEE Access*, vol. 6, pp. 27465–27472, 2018, doi: 10.1109/ACCESS.2018.2833841.

JIA LI received the M.Sc. degree from Kumamoto University, Kumamoto, Japan, in 2011, and the Ph.D. degree in engineering from Jilin University, Changchun, China, in 2019. She is currently a Lecturer with the Department of Intelligent Manufacturing, Kumamoto University. Her research interests include digital image and biomedical signal processing, feature extracting, and classification in artificial intelligence.

YANG ZHANG received the master's degree from the South China University of Technology, Guangzhou, China, in 2019. He is currently a Teacher with the Zhuhai College of Jilin University, Zhuhai, China. His research interests include digital image processing, biomedical signal processing, and machine learning.

LE GAO received the Ph.D. degree in big data technology from the National Supercomputer Center, Guangzhou, China, in 2018. He is currently a Distinguished Professor with Wuyi University, Jiangmen, China. He has published more than 20 articles. His research interests include big data technology, big data application, and machine learning.

XIANG LI (Member, IEEE) received the doctor's degree from Okayama University, Japan, in 2019. He is currently an Associate Professor with the Zhuhai College of Jilin University. He presided over the projects of walking control of humanoid robot based on stereo vision and automatic charging system of underwater robot based on stereo vision servo. His research interests include machine vision and underwater robot control.